

Leaf, plant, to canopy: A mechanistic study on aboveground plasticity and plant density within a maize–soybean intercrop system for the Midwest, USA

Elena A. Pelech¹  | Jochem B. Evers²  | Taylor L. Pederson¹ |
David W. Drag¹  | Peng Fu³  | Carl J. Bernacchi^{1,4} 

¹The Carl R. Woese Institute for Genomic Biology, University of Illinois at Urbana-Champaign, Urbana, Illinois

²Department of Plant Sciences, Centre for Crop Systems Analysis, Wageningen University, Wageningen, The Netherlands

³Center for Environment, Energy, and Economy, Harrisburg University of Science and Technology, Harrisburg, Pennsylvania, USA

⁴USDA-ARS Global Change and Photosynthesis Research Unit, Urbana, Illinois, USA

Correspondence

Carl J. Bernacchi, 1201W. Gregory Dr, Urbana, IL 61801, USA
Email: carl.bernacchi@usda.gov

Funding information

Agricultural Research Service; U.S. Department of Agriculture

Abstract

Plants have evolved to adapt to their neighbours through plastic trait responses. In intercrop systems, plant growth occurs at different spatial and temporal dimensions, creating a competitive light environment where aboveground plasticity may support complementarity in light-use efficiency, realizing yield gains per unit area compared with monoculture systems. Physiological and architectural plasticity including the consequences for light-use efficiency and yield in a maize-soybean solar corridor intercrop system was compared, empirically, with the standard monoculture systems of the Midwest, USA. The impact of reducing maize plant density on yield was investigated in the following year. Intercropped maize favoured physiological plasticity over architectural plasticity, which maintained harvest index (HI) but reduced light interception efficiency (ϵ_i) and conversion efficiency (ϵ_c). Intercropped soybean invested in both plasticity responses, which maintained ϵ_i , but HI and ϵ_c decreased. Reducing maize plant density within the solar corridor rows did not improve yields under monoculture and intercrop systems. Overall, the intercrop decreased land-use efficiency by 9%–19% and uncoordinated investment in aboveground plasticity by each crop under high maize plant density does not support complementarity in light-use efficiency. Nonetheless, the mechanistic understanding gained from this study may improve crop cultivars and intercrop designs for the Midwest to increase yield.

KEYWORDS

complementarity, light-use efficiency, plant architecture, yield

1 | INTRODUCTION

Predicted increases in global population growth and economic development coupled with decreases in land resources and biodiversity have fostered attention in agroecological approaches for a

sustainable intensification of agriculture (Foley et al., 2011; Godfray & Garnett, 2014; Tilman et al., 2011, 2017). Polycultures, or the commonly used term intercropping, is an ancient and indigenous agroecological approach defined as the simultaneous or relay cultivation of multiple crops on the same field during a significant

This is an open access article under the terms of the Creative Commons Attribution-NonCommercial License, which permits use, distribution and reproduction in any medium, provided the original work is properly cited and is not used for commercial purposes.

© 2022 The Authors. *Plant, Cell & Environment* published by John Wiley & Sons Ltd. This article has been contributed to by U.S. Government employees and their work is in the public domain in the USA.

part of their growth cycle (Vandermeer, 1989; Zaem et al., 2019). Compared with the cultivation of single crops (monocultures hereafter), intercropping has demonstrated increases in crop production per unit land area with improvements in regulating ecosystem services (Brooker et al., 2015; Cong et al., 2015; S. Li et al., 2020). Evolving intercrop designs for agroecosystems where intercropping is not the dominant form of agriculture, such as the Midwest, USA, remains restricted by mechanized management with existing machinery. Intercropping designs that can be mechanized may also demonstrate higher yields on a land area basis with additional ecosystem services relative to the standard regional practice.

The Midwest, USA, is commonly managed by an annual rotation between maize (*Zea mays* L.) and soybean (*Glycine max* L. Merr.) monocultures representing 30%–40% of the global production (FAO, 2020). There is interest among Midwestern farmers in intercropping N-fixing legumes between maize rows that are wider-spaced (2×) and at equal maize planting density compared with the standard maize monoculture (Abels et al., 2019; Kremer, 2016; Kremer & Deichman, 2014b). Maize arranged in the wide rows, defined as a solar corridor, may improve yields by maximizing the availability of incident light deeper into the canopy (Deichman, 2000; Kremer, 2016; Kremer & Deichman, 2014b). The legume, with the added benefit of biological N fixation, can provide forage for grazing livestock after mechanical maize harvest or be used as a crop residue to improve soil fertility for succeeding crops in rotation (Abels et al., 2019; Kremer & Deichman, 2014a).

The maximal yield potential of crops based on the availability of incident light is determined by the interception efficiency (ϵ_i), conversion efficiency (ϵ_c), and harvest index (HI) (Monteith & Moss, 1977). The rate and duration of canopy closure paired with canopy size and architecture affect ϵ_i , whereas ϵ_c defines how efficiently the intercepted light is converted into biomass by balancing photosynthetic carbon gain and respiratory carbon loss. The HI represents the fraction of total aboveground biomass partitioned to harvestable organs. An assumption of high-performing cultivars in monocultures is that the theoretical maximum of ϵ_i and HI have already been achieved (Koester et al., 2014; Zhu et al., 2010), whereas lesser gains in ϵ_c for C_3 and C_4 crops have been realized (Zhu et al., 2008). Therefore, maintaining these efficiencies for each species in the solar corridor intercrop system may collectively lead to greater light capture and use, resulting in a yield advantage on a land area basis over the standard maize monoculture.

However, plant growth of different species occurs at different temporal and spatial dimensions, which creates a competitive light environment in intercrops. In response, plants can adapt to the proximity of neighbours by inducing plastic responses and establish resource complementarity with their neighbours (Cardinale et al., 2007; Li et al., 2014; Loreau & Hector, 2001; Niklaus et al., 2017). Within the solar corridor, the structural dominance of maize planted in the north–south row direction may significantly decrease incident light for the intercropped legume during the morning and afternoon when the solar elevation angles are low. Thus, the legume may maximize net carbon gain through increased chlorophyll content,

specific leaf area (SLA) and reduced chlorophyll α/b ratio (physiological plasticity), or the legume may minimize shading by branch reduction, and stem and petiole elongation (architectural plasticity). These plastic responses are also referred to as shade tolerance and shade avoidance, respectively (Boardman, 1977; Givnish, 1988; Gommers et al., 2013; Gong et al., 2015; Valladares & Niinemets, 2008). If investment in these aboveground plasticity responses leads to a significant biomass accumulation in the legume, more far-red light than red light will be reflected upwards, which may induce neighbour proximity signals and subsequent plasticity responses in maize (Zhang et al., 2020a, 2020b). In addition, intraspecific competition may occur between maize plants by the doubling of plant density within the solar corridor rows, which may offset any improvement in light distribution expected from the wider row widths. Therefore, characterizing the degree of aboveground plasticity in both species in the solar corridor intercrop system can provide a mechanistic understanding of how light complementarity and yield advantages might be realized, which could aid future trait selection and breeding.

The extent of physiological and architectural plasticity and its consequences for the three seasonal light-use efficiencies and yield within a maize and soybean solar corridor intercrop system were evaluated against respective monoculture systems under a constant maize plant density during the 2019 growing season. In the following year, maize plant density treatments in the solar corridor row configuration were investigated to determine whether reducing maize plant density eases competition and establishes a yield advantage compared with the standard maize monoculture. These field experiments were used to translate the ecophysiological complexities within an intercrop system from the leaf, plant, and canopy, which may highlight key factors to improve crop production beyond the standard monoculture systems of the Midwest, USA.

2 | METHODS

2.1 | Site description

Field experiments were conducted at the Energy Farm, University of Illinois at Urbana-Champaign (40°03'N, 88°12', 215 m above sea level) during the 2019 and 2020 growing seasons. Soils at the experimental site are Drummer silty clay loam (Typic Endoaquolls) that is deep and poorly drained (Soil Survey Staff, 2015). Preplanting soil properties included 3.2% organic matter, pH 5.8, 67.3 kg P ha⁻¹, 335.1 kg K ha⁻¹, 4919.4 kg Ca ha⁻¹ and 881.0 kg Mg ha⁻¹. The site previously maintained a 2-year rotation of maize and soybean monocultures, where no nitrogen fertilizer was added before or after soybean planting, which is in accordance with the standard practice of the region. Both experimental years used the same cultivars: hybrid maize (*Z. mays* L. [DEKALB DKC63-21RIB]) and indeterminate soybean (*G. max* L. Merr. [Asgrow AG36X6]).

In 2019, experimental plots were arranged in a randomized complete block design with four replicates (Appendix Figure A.1). Maize and soybean were sown simultaneously on June 3 under both monoculture and solar corridor cropping systems with a six-row seed drill planter using planting densities typically used in the Midwestern USA. All experimental plots consisted of north–south rows recommended for the solar corridor intercrop system (Deichman, 2000; Appendix Figure A.1). The monoculture plots consisted of three cropping systems as follows: (i) 12 soybean rows with a row spacing of 0.76 m at a planting density of 34.6 plants m^{-2} (soybean monoculture, $M_{soybean}$); (ii) 12 maize rows with a row spacing of 0.76 m at a planting density of 8.4 plants m^{-2} (maize monoculture, M_{maize}); (iii) 6 maize rows with a row spacing of 1.52 m at a planting density of 16.8 plants m^{-2} (solar corridor maize monoculture, $sc.M_{maize}$). The solar corridor intercropped plots consisted of 12 alternating rows of maize ($sc.I_{maize}$) and soybean ($sc.I_{soybean}$) at 0.76 m row spacing, and at equal planting densities as $sc.M_{maize}$ and $M_{soybean}$, respectively (Figure 1a). Explicitly, the intercrop holds an additive design compared with the maize monocultures, but $sc.I_{soybean}$ holds a replacement design by $\frac{1}{2}$ compared with $M_{soybean}$. In 2020, the experimental plots from 2019 were repeated, except (1) there were three replicate blocks, (2) there were two additional maize density treatments for $sc.M_{maize}$ and $sc.I_{maize}$ at lower planting densities than

M_{maize} , and (3) maize was planted with a precision vacuum seed planter (Appendix Figure A.1).

In both years, 202 kg N ha^{-1} as urea granules (ESN, Smart Nitrogen) was side dressed to all maize rows across experimental plots at early vegetative growth (three maize leaves) to maximize the potential for soybean nodulation in the intercrop plots. Daily temperature and precipitation data over the growing season from planting to harvest were obtained from the mean of three weather stations on-site and daily solar radiation ($MJ m^{-2}$) was measured over the experimental plots (Figure 2). Plots were harvested at physiological maturity (Table 1).

2.2 | Leaf tissue sampling

Leaf tissue sampling measured the degree of physiological plasticity. During the 2019 growing season, leaf disks (1 cm diameter) were collected from fully developed leaves at the top of the canopy around solar noon to determine chlorophyll content (chl content), chlorophyll a/b ratios (chl a/b), and carotenoid content (Lichtenthaler, 1987; Porra et al., 1989). Three leaf disks (1.8 cm in diameter) were also collected and then dried at 60°C to determine SLA ($mm^2 mg^{-1}$). The dried samples were then ground to a powder, after which a target

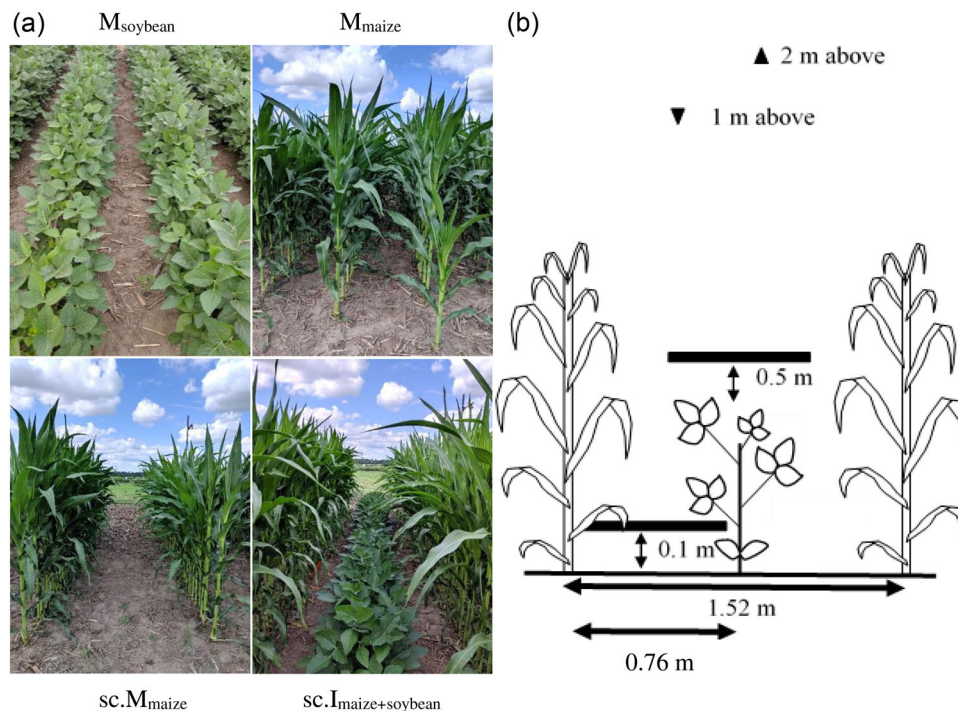


FIGURE 1 Cropping systems and quantum sensor placement during the 2019 growing season. (a) Representative photograph of the four cropping systems taken on 22 July 2019 (42 days after emergence [DAE]): soybean monoculture at 0.76 m row space ($M_{soybean}$), maize monoculture at 0.76 m row space (M_{maize}), solar corridor maize monoculture at 1.52 m row space ($sc.M_{maize}$), and solar corridor intercrop at 0.76 m row space ($sc.I_{maize+soybean}$). The within-row maize plant density is doubled in both solar corridor systems to maintain plant density to M_{maize} . The $sc.I_{maize+soybean}$ system had half the number of soybean rows compared to $M_{soybean}$. All rows were north–south orientation. (b) Illustrative representation of the $sc.I_{maize+soybean}$ system. Rectangular bars indicate the placement of line quantum sensors, inverted triangle indicates the placement of a point sensor measuring upwelling light and the upright triangle indicates the placement of a point sensor measuring downwelling light. Figure is not to scale.

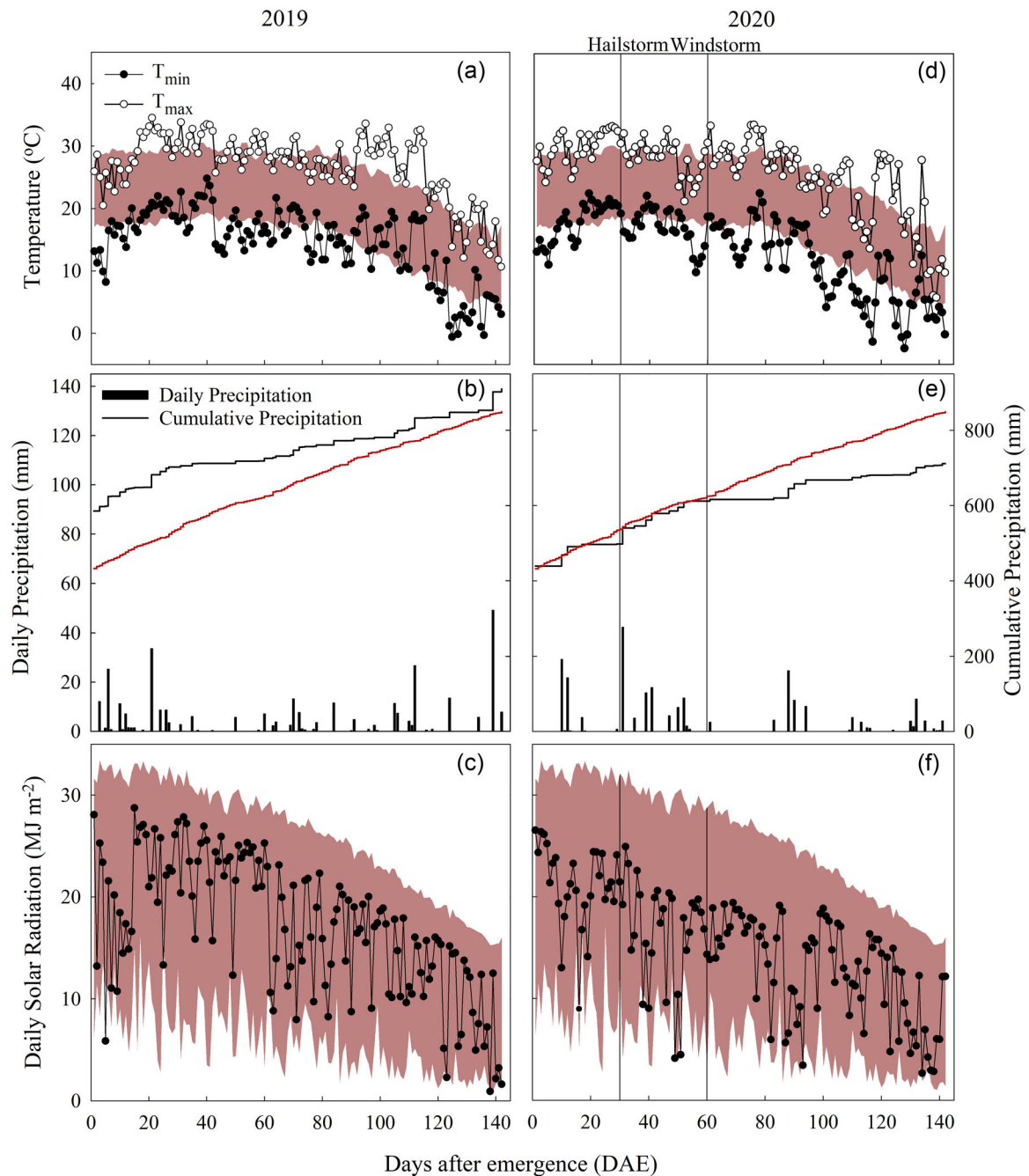


FIGURE 2 Meteorological conditions across the 2019 and 2020 growing seasons in Champaign, IL, USA. Daily observations are indicated for maximum (white circle) and minimum (black circle) air temperatures with the 30-year mean temperature ranges (red band) AD, daily (black bar) and cumulative precipitation (black line) with the cumulative 30-year mean precipitation (red line) BE and daily incident solar radiation (black circle) with the 30-year mean incident solar radiation range (red band) CF. The vertical lines represent each storm that occurred during the 2020 growing seasons where the hailstorm and windstorm (derecho) occurred at 30 and 60 days after emergence (DAE), respectively. Historical weather data were obtained from the Illinois Climate Network (10.13012/J8MW2F2Q). [Color figure can be viewed at [wileyonlinelibrary.com](https://onlinelibrary.wiley.com)]

mass of 2–4 mg was weighed and combusted with oxygen in an elemental analyser (Costech 4010; Costech Analytical Technologies), which was calibrated to %N against an acetanilide standard curve to determine carbon to nitrogen ratios (C:N). Samples were collected four times during the growing season between vegetative and reproductive growth stages for both maize and soybean for a temporal picture of the degree of physiological plasticity.

2.3 | Plant architecture analysis

Plant architecture analysis measured the degree of architectural plasticity. The phytomer was used as the primary ranking unit for the architectural analysis of maize and soybean plants (Appendix Figure A.3 and A.4). Nondestructive measurements of phytomer development were conducted during the 2019 growing season on three maize and four soybean

TABLE 1 Summary of maize and soybean cropping systems and corresponding row space, planting dates, harvest dates and final plant densities during the 2019 and 2020 growing season

Year	Cropping system	Row space ^a (m)	Planting date	Emergence date	Harvest date	Final plant density ^b (plants/m ²)
2019	Maize monoculture (M_{maize})	0.76	3 Jun	10 Jun	15 Oct	6
	Maize solar corridor monoculture ($sc.M_{\text{maize}}$)	1.52				
	Maize solar corridor intercrop ($sc.I_{\text{maize}}$)	1.52				
	Soybean monoculture (M_{soybean})	0.76	3 Jun	10 Jun	15 Oct	22
	Soybean solar corridor intercrop ($sc.I_{\text{soybean}}$)	1.52			28 Oct	11
2020	Maize monoculture (M_{maize})	0.76	2 Jun	12 Jun	15 Oct	5
	Maize solar corridor monoculture ($sc.M_{\text{maize}}$)	1.52				5, 4, 3
	Maize solar corridor intercrop ($sc.I_{\text{maize}}$)	1.52				5, 4, 3
	Soybean monoculture (M_{soybean})	0.76	3 Jun	12 Jun	20 Oct	18
	Soybean solar corridor intercrop ($sc.I_{\text{soybean}}$)	1.52				9

^aRow space within species.

^bFinal plant density is the average plant stand after germination and the 2020 windstorm (derecho).

plants in each plot, which were tagged at emergence. Internode length, petiole length, and plant height were measured with a ruler, leaf/blade dimensions were measured with a handheld leaf area metre (CI-203, CID Bio-science) and soybean pod number at reproductive stages were counted. Measurements were conducted every week through to silking and full pod for maize and soybean, respectively. Given the importance of maintaining nondestructive measurements, maize internode and sheath length could not be measured. Therefore, the distance between blade collars was measured instead, where Phytomer 1 was defined as the first leaf blade after the cotyledon. If occurred, soybean branching at the lower phytomers was considered a single phytomer where petiole length was measured as the distance between the node at the base of the stem to the last branching petiole. The last sampling time point was considered the final organ size and used for comparison in this study where soybean Phytomer 1 (unifoliate leaves) and maize Phytomers 1–5 are excluded due to their advanced senescence.

2.4 | Light response of leaf photosynthesis

In 2019, photosynthetic light response curves were conducted around solar noon on the youngest fully expanded leaf at silking for maize and the beginning of seed production for soybean. All measurements were conducted with open path gas exchange systems equipped with a leaf chamber fluorometer of 6 cm² (LI-6800, LI-COR). Curves consisted of 12 points from 2000 to 0 $\mu\text{mol m}^{-2} \text{s}^{-1}$ photosynthetic photon flux density (PPFD) following acclimation at 2000 $\mu\text{mol m}^{-2} \text{s}^{-1}$ PPFD. Leaves were acclimated to full sunlight to mimic the environmental conditions outside of the chamber (Figure 3). Chamber conditions were set to 60%–80% humidity, ambient air temperature (determined by T_{air} °C with open leaf chamber), and 410 p.p.m. reference CO₂ concentration in the airstream. Response curves were fitted using an Excel-based fitting tool (Bellasio et al., 2015, 2016) to derive:

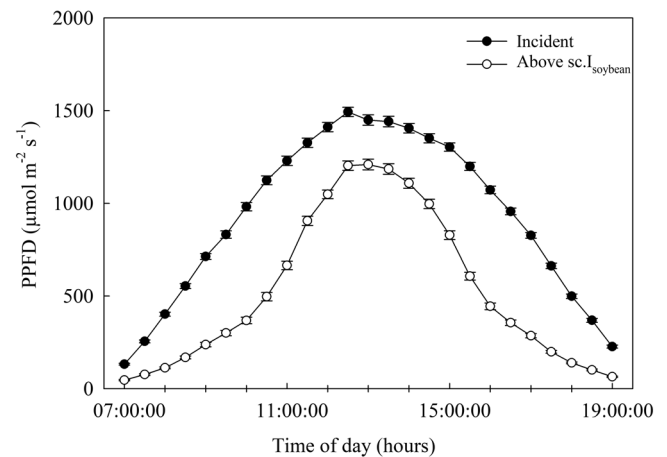


FIGURE 3 Shade conditions for intercropped soybean during the 2019 growing season. Mean photosynthetic photon flux density (PPFD) incident and above intercropped soybean between wide maize rows in the solar corridor arrangement ($sc.I_{\text{soybean}}$) during sunlight hours (07:00 a.m.–07:00 p.m.). Each point represents a 30 min interval of the day averaged across 75 measurement days. Error bars represent ± 1 SE error of the mean and $n = 4$ for all data points. Rows were north–south orientation.

(i) maximum rate of photosynthesis (A_{sat}) by fitting a nonrectangular hyperbola; (ii) apparent quantum yield (AQY) by the initial linear slope of the fitted curve; (iii) PPFD-A compensation point (LCP); and (iv) dark respiration (R_d).

2.5 | Biomass determination

Aboveground biomass harvests were conducted four times at 2–3 week intervals during the 2019 growing season across vegetative and

reproductive growth stages of maize and soybean. A 1 m length of a row in each plot was harvested at soil level while avoiding plot borders and previously harvested locations. The number of plants per metre was recorded and the total leaf area per plant was determined for three harvested plants using a leaf area metre (CI-203CA, CID Bio-science). Stems (including petioles and petiolules or sheaths), leaves and pods or cobs were then separated and dried at 60°C for a minimum of 1 week to determine dry weights. To convert total biomass into total energy content (MJ m^{-2}) for the calculation of conversion efficiency (ϵ_c), the separated organs were ground and analysed using adiabatic bomb calorimetry (Model 6200, Parr Instrument).

2.6 | Seasonal interception efficiency and conversion efficiency

Daily canopy light interception fractions and seasonal interception efficiency (ϵ_i) during the 2019 growing season were calculated as,

$$\epsilon_i = 1 - \left(\frac{l_t + l_r}{l_o} \right) \quad (1)$$

where l_o was incident PPFD ($\mu\text{mol m}^{-2} \text{s}^{-1}$) measured above the canopy with a downwelling quantum point sensor 2 m above canopy surface, l_t was transmitted PPFD ($\mu\text{mol m}^{-2} \text{s}^{-1}$) measured at 0.1 m from the soil surface using a quantum line sensor, and l_r was reflected PPFD ($\mu\text{mol m}^{-2} \text{s}^{-1}$) measured with an upwelling quantum point sensor 1 m above the canopy surface. A line quantum sensor was also placed 0.5 m above the soybean row in the intercrop systems to partition interception fractions within the canopy (Figure 1b and Appendix Figure A.5).

All measurements were collected using point (Model SQ-215) and line (Model SQ-311) quantum sensors (Apogee Instruments). All data were logged every 15 s and averaged over 30 min using a datalogger (model CR1000 with AM16/32B multiplexer, Campbell Scientific). Measurements began 23 days after emergence (DAE) at early vegetative growth for maize and soybean. All sensors were factory calibrated. Data were checked for errors daily and sensor height was adjusted weekly to maintain their constant distance from the growing canopy surface. Data loss from storm damage, equipment failure, or power outage represented <3.5% of total data collection. Where gaps existed, data from plots within the same treatment were averaged to fill the missing data gaps.

The slope of linear fit of cumulative absorbed photosynthetically active radiation (APAR [MJ m^{-2}]) versus cumulative biomass energy (MJ m^{-2}) was used to estimate conversion efficiency (ϵ_c) where APAR was calculated as

$$\text{APAR} = l_o - (l_t + l_r) \quad (2)$$

2.7 | Yield

In both experimental years, total aboveground biomass at physiological maturity was measured by harvesting 3 m from the centre rows

per plot by hand, to determine grain yield, stover, HI and seed mass. The 2019 grain yield data were used to calculate the Land Equivalent Ratio (LER; Vandermeer, 1989) to assess the land-use efficiency

$$\text{LER} = \frac{Y_{\text{sc.l maize}}}{Y_{\text{Mmaize}}} + \frac{Y_{\text{sc.l soybean}}}{Y_{\text{Msoybean}}}, \quad (3)$$

where Y is the yield (g m^{-2}) of maize or soybean in the corresponding system indicated by the subscripts. If $\text{LER} > 1$, the intercrop system has a yield advantage and increased land-use efficiency per unit area compared with the monocultures. The 2020 grain yield data from cropping systems with the highest maize plant density was used to calculate a 2-year average LER ($\text{LER}_{\text{average}}$) by using the equation above. In addition, an LER if the solar corridor intercrop were to replace the maize monoculture in the standard annual rotation of the Midwest, USA, was also calculated,

$$\text{LER}_{\text{rotation}} = \frac{Y_{\text{Msoybean}} \leftrightarrow Y_{\text{sc.l maize+soybean}}}{Y_{\text{Mmaize}} \leftrightarrow Y_{\text{Msoybean}}}, \quad (4)$$

where Y was the average yield (g m^{-2}) of the rotation between 2019 and 2020, represented by the \leftrightarrow symbol. Specifically, the numerator represents the average yield of the annual rotation with the solar corridor intercrop and the denominator represents the standard annual rotation between maize and soybean monocultures. The LER per possible rotation scenario were averaged to produce $\text{LER}_{\text{rotation}}$ ($n = 4$).

2.8 | Data and statistical analysis

In the calculation of the 2-year average grain yield for each cropping system, the third block in 2019 was omitted to equal the number of replicate blocks between years and include each border block. As the plant density of $\text{sc.l}_{\text{soybean}}$ is half compared with the plant density of $\text{M}_{\text{soybean}}$ (Table 1), analysis of ϵ_i and ϵ_c from 2019 were normalized to the area of $\text{sc.l}_{\text{soybean}}$ to make meaningful comparisons by multiplying the $\text{M}_{\text{soybean}}$ averages by 0.5, abbreviated as $\text{M}_{\text{soybean}}^{*0.5}$. Likewise, $\text{M}_{\text{soybean}}$ grain yield (g m^{-2}) was also multiplied by 0.5 in both years to give the expected yield under the null hypothesis that an individual soybean plant has the same yield in the intercrop and monoculture (Loreau & Hector, 2001). The observed $\text{sc.l}_{\text{soybean}}$ yield was then compared with the expected yield, where a decrease indicates a yield loss for intercropped soybean.

Statistical analyses were conducted on the plot means using a mixed model analysis of variance using R software (R Core Team, 2021) and the lme function (package 'nlme', Pinheiro et al., 2021) with cropping system considered fixed effects and block and block by cropping system effects considered random. SLA, chl content, chl a/b, carotenoid content, C:N, biomass, plant height and leaf area per plant measured in 2019 were analysed as repeated measures with DAE as the repeated fixed factor. First-order linear regressions for the calculation of ϵ_c were performed on each replicate block, where $n = 4$ (SigmaPlot, Systat Software). All statistical analyses were conducted within species, except for the parameters in Figure 9.

Multiple pairwise comparisons of maize treatments were conducted using the emmeans function (package 'emmeans', Russell, 2021). The residuals were checked for normality and constant variance, and an α of 0.1 was used to determine significance and reduce the probability of Type II errors.

3 | RESULTS

3.1 | Meteorological conditions during the 2019 and 2020 growing season

The majority of daily maximum and minimum air temperatures were higher than the daily 30-year mean temperature ranges in both years (Figure 2a,d). At emergence in 2019, the cumulative precipitation rate was higher than the 30-year mean, but by the end of the season both rates were similar, and so 200 mm less precipitation fell across the 2019 growing season compared with the 30-year mean (Figure 2b). In contrast, the cumulative precipitation rate at emergence in 2020 matched the 30-year mean, but less precipitation fell across the season (Figure 2e). Daily incident solar radiation across each growing season fell within the 30-year mean range (Figure 2c,f). Two destructive weather events occurred in 2020, a hailstorm and windstorm (derecho) at 30 and 60 DAE, respectively. The hailstorm caused significant damage to plant architecture, where corn smut galls developed by the pathogenic fungus *Ustilago maydis* in maize, and the windstorm decreased the original maize plant density treatments by 1 and 4 plants per m² on average for maize and soybean, respectively (Appendix Figure A.2 and Table 1).

3.2 | The intercrop system provided 65%–80% of incident light for understory soybean around solar noon in 2019

The solar corridor arrangement of maize rows running north–south provided 35% of incident light (expressed as PPFD [$\mu\text{mol m}^{-2} \text{s}^{-1}$]) to sc.l_{soybean} during the morning before an increase to approximately 80% at solar noon (13:00), before decreasing back to 35% in the afternoon (Figure 3). Thus, the solar corridor intercrop system provided 65%–80% of incident light for soybean between maize rows ± 2 h from solar noon in 2019.

3.3 | Intercropping increased SLA by 24% while maintaining light-use efficiency at the leaf level for soybean

Soybean SLA in both cropping systems declined with development (Figure 4a and Appendix Table A.1). Intercropping increased soybean SLA for all sampling days (Figure 4a) in addition to the seasonal mean by ~24% ($p < 0.001$, Table 2). In contrast, soybean total chl content increased with development (Figure 4b). There was a significant DAE

by cropping system interaction for soybean total chl content (Appendix Table A.1) and was greater for M_{soybean} than sc.l_{soybean} at 67 DAE, which corresponds to the beginning of seed production ($p < 0.1$, Figure 4b). Across the season, total chl content was similar between soybean treatments ($p = 0.11$, Table 2); however, chl a/b ratios for sc.l_{soybean} was lower than M_{soybean} on all sampling days (Figure 4d) and across the growing season (Table 2, $p < 0.05$). There was a significant DAE by cropping system interaction on soybean carotenoid content (Appendix Table A.1). Intercropping decreased carotenoid content for soybean after full bloom at 38 DAE and across the season by 19% compared with M_{soybean} (Figure 4c and Table 2, $p < 0.05$). Likewise, the average C:N ratio for sc.l_{soybean} was lower at 38 DAE (Appendix Table A.1 and Figure 4e) and seasonally (Table 2, $p < 0.05$). Intercropping soybean significantly decreased all photosynthetic parameters of light response curves compared with M_{soybean} ($p < 0.1$), except for the AQY ($p = 0.41$, Table 3), demonstrating similar AQY at the leaf level.

3.4 | Soybean architecture varied between cropping systems

Intercropped soybean plants had significantly greater final internode length than M_{soybean} plants between phytomer Ranks 2 and 13, and the remaining 2 uppermost phytomers were significantly higher for M_{soybean} ($p < 0.05$; Figure 5a). This result corresponds to the significant increases in sc.l_{soybean} plant height by ~10% across development compared with M_{soybean} plant height (Appendix Table A.1 and Figure A.6A). The final petiole length and total leaf area between Ranks 2–5 and 2–6, respectively, for M_{soybean} were greater than sc.l_{soybean} plants due to branching by M_{soybean} plants ($p < 0.1$, Figure 5b,c and Appendix Figure A.9). For the remaining ranks, petiole length and total leaf area at the middle phytomers had no significant differences, except Rank 8 was higher for sc.l_{soybean} ($p < 0.1$, Figure 5b,c) and the upper phytomers were greater for M_{soybean} ($p < 0.1$, Figure 5b,c). Consequently, the majority of phytomer ranks for sc.l_{soybean} plants had significantly fewer pods than M_{soybean}, with the greatest difference at the lower phytomer ranks where branching occurred in M_{soybean} plants ($p < 0.1$, Figure 5d).

3.5 | Intercropping increased SLA and decreased chl content without impacting photosynthesis for maize

At 52 DAE, SLA of sc.M_{maize} was higher than M_{maize} ($p < 0.1$, Figure 4f). Later in reproductive development at 80 DAE, SLA of sc.l_{maize} was higher than both maize monocultures ($p < 0.1$, Figure 4f). Seasonally, however, only SLA of sc.l_{maize} was significantly higher than M_{maize} by ~10% ($p < 0.05$, Table 2). On individual sampling days, no differences in total chl content were observed between maize cropping systems (Figure 4g), but seasonally, sc.l_{maize} chl content was

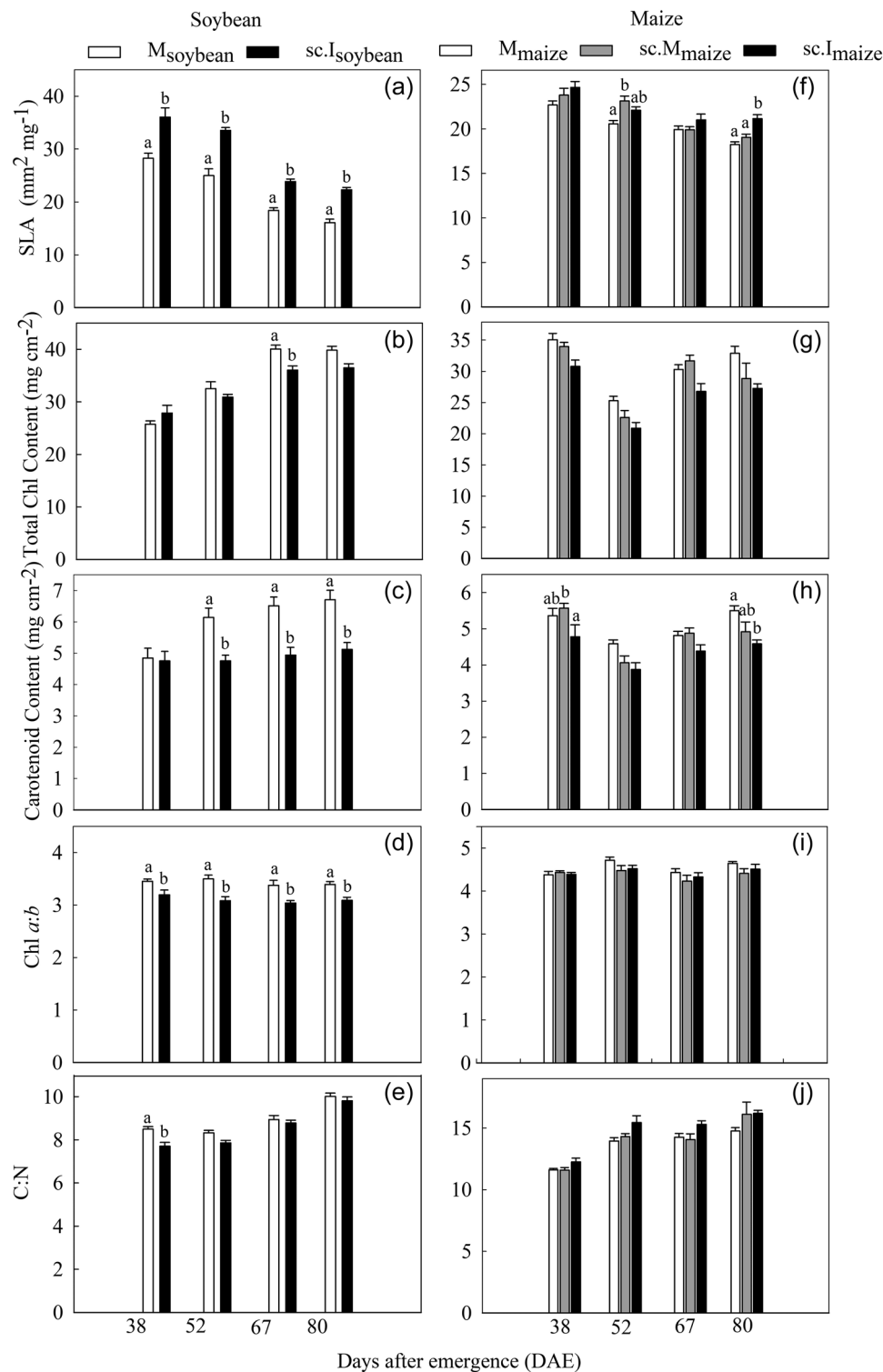


FIGURE 4 Tissue sampling analysis across multiple days after emergence (DAE) during the 2019 growing season. Mean specific leaf area (SLA) AF, total chl content BG, carotenoid content CH, chl a:b DI and C:N EJ for soybean in monoculture (M_{soybean} = white bars) and solar corridor intercrop ($sc.I_{\text{soybean}}$ = black bars), and maize in monoculture (M_{maize} = white bars), solar corridor monoculture ($sc.M_{\text{maize}}$ = grey bars) and solar corridor intercrop ($sc.I_{\text{maize}}$ = black bars). Error bars and replicates are as in Figure 3. Letters indicate significant differences within DAE at $\alpha = 0.1$.

lower than M_{maize} by 15% ($p < 0.1$, Table 2). Likewise, no differences in chl a/b ratios were found between maize cropping systems on individual sampling days (Figure 4i), but seasonally, $sc.M_{\text{maize}}$ was lower than M_{maize} ($p < 0.1$, Table 2). For carotenoid content, $sc.I_{\text{maize}}$

was lower than M_{maize} later in reproductive development at 80 DAE ($p < 0.1$, Figure 4h). Alternatively, $sc.M_{\text{maize}}$ carotenoid content was higher than $sc.I_{\text{maize}}$ early in development at 38 DAE ($p < 0.1$, Figure 4h). Seasonally, carotenoid content was 13% lower for $sc.I_{\text{maize}}$

TABLE 2 Seasonal averages of SLA, C:N and leaf pigments of maize and soybean in monoculture and intercrop systems during the 2019 growing season

Parameter		Maize				Soybean		
		M	sc.M	sc.I	MSE	M	sc.I	MSE
SLA	mm ² mg ⁻¹	20.36 ± 0.30	21.48 ± 0.39	22.23 ^a ± 0.34	0.91	21.93 ± 0.84	28.94 ^a ± 0.98	2.83
Total Chl content	µg cm ⁻²	30.88 ± 0.70	29.42 ± 0.95	26.44 ^a ± 0.71	0.0007	34.54 ± 0.97	32.83 ± 0.70	0.0003
Chl a:b	-	4.54 ± 0.04	4.39 ^a ± 0.05	4.44 ± 0.04	0.02	3.43 ± 0.03	3.10 ^a ± 0.03	0.01
Carotenoid content	µg cm ⁻²	5.07 ± 0.09	4.87 ± 0.12	4.41 ^a ± 0.12	0.13	6.05 ± 0.18	4.89 ^a ± 0.12	0.29
C:N	-	13.64 ± 0.22	14.02 ± 0.37	14.79 ± 0.28	0.0001	8.94 ± 0.12	8.54 ^a ± 0.14	0.08

Note: 2019 growing season means ± 1 SE ($n = 4$) are reported for SLA, total chlorophyll content, carotenoid content, chlorophyll a:b ratio and C:N. Leaf sampling was conducted four times between vegetative and reproductive growth stages for both maize and soybean. MSE is reported from each ANOVA. Abbreviations: ANOVA, analysis of variance; C:N, carbon to nitrogen ratio; MSE, Mean square error; SLA, specific leaf area.

^aSignificant differences compared with M are indicated at $\alpha = 0.1$.

TABLE 3 Estimates from leaf photosynthetic light response curves of maize and soybean in monoculture and intercrop systems during the 2019 growing season

Parameter		Maize				Soybean		
		M	sc.M	sc.I	MSE	M	sc.I	MSE
A _{sat}	µmol m ⁻² s ⁻¹	56.19 ± 2.70	50.40 ± 1.86	48.82 ± 1.73	13.95	37.7 ± 1.62	29.89 ^a ± 1.12	7.56
AQY	-	0.068 ± 0.002	0.065 ± 0.002	0.064 ± 0.002	0.0001	0.055 ± 0.001	0.054 ± 0.001	0.0001
LCP	µmol m ⁻² s ⁻¹	59.33 ± 2.95	51.61 ± 2.29	55.37 ± 3.16	12.77	53.89 ± 2.25	34.27 ^a ± 1.45	5.50
R _d	µmol m ⁻² s ⁻¹	3.94 ± 0.27	3.29 ± 0.18	3.46 ± 0.16	0.0001	2.91 ± 0.13	1.83 ^a ± 0.08	0.013

Note: Cropping system means ± 1 SE ($n = 4$) are reported for parameters related to photosynthetic light curves (Appendix Figure A.10). Curves were conducted in 2019 at silking and beginning of seed production for maize and soybean, respectively. MSE is reported from each ANOVA.

Abbreviations: ANOVA, analysis of variance; MSE, mean square error.

^aSignificant differences compared with M are indicated with an asterisk at $\alpha = 0.1$.

compared with M_{maize} ($p < 0.05$). Maize cropping system treatments did not affect C:N ratios ($p > 0.1$, Figure 4j and Table 2) and photosynthetic light response parameters ($p > 0.1$, Table 3). There were no interacting effects for any maize leaf tissue analysis parameters (Appendix Table A.1).

3.6 | The solar corridor row arrangement decreased blade width of maize

At silking, maize in both solar corridor treatments had a maximum of 16 leaves (phytomers), whereas M_{maize} had a total of 17. Across all maize cropping system treatments, leaves positioned at the middle of the plant (Phytomers 7–10) had the greatest blade length and successive leaves displayed a steady decline (Figure 6a). Before the peak in blade length at Phytomer 10, blade length of both sc.M_{maize} and sc.I_{maize} were longer than M_{maize} by 7%–10% ($p < 0.001$). Beyond Rank 10, sc.I_{maize} decreased in blade length between Ranks 13 and 16 compared with M_{maize} by 20%–136% ($p < 0.1$). Consequently, these phytomer ranks also showed a similar decrease in sc.I_{maize} blade area ($p < 0.1$, Figure 6c). Among all maize treatments, blade width peaked between phytomer Ranks 9 and 12 before a steady decline for the upper leaf positions (Figure 6b). For phytomer Ranks 8 through 16, M_{maize} plants had wider leaf blades by

7%–142% compared with sc.I_{maize} with 5 of those ranks also wider than sc.M_{maize} plants ($p < 0.1$).

The distance between leaf blade collars had a varied response between maize cropping systems (Figure 6d). For the majority of the upper phytomer ranks, sc.I_{maize} had smaller distances than M_{maize} by 5%–18% ($p < 0.1$, Figure 6d), which corresponds to the significant decreases in sc.I_{maize} final plant height compared to M_{maize} (Appendix Table A.1 and Supporting Information: Figure S4B). Distances between blade collars for sc.M_{maize} fell between M_{maize} and sc.I_{maize} (Figure 6d), and thus no differences in sc.M_{maize} plant height was found (Appendix Table A.1 and Figure A.4B).

3.7 | Intercropping decreased maize plant leaf area but did not impact soybean plant leaf area

The average plant leaf area of sc.I_{soybean} was slightly higher than M_{soybean} at 30 DAE (Figure 7a) and the greater light interception fractions for sc.I_{soybean} early in canopy development reflects this initial increase (Figure 7b). From full bloom onwards (40 DAE), sc.I_{soybean} plant leaf area was slightly lower than M_{soybean} plants. However, statistically, there was no significant cropping system effect across development ($p = 0.28$) and soybean plant leaf area was

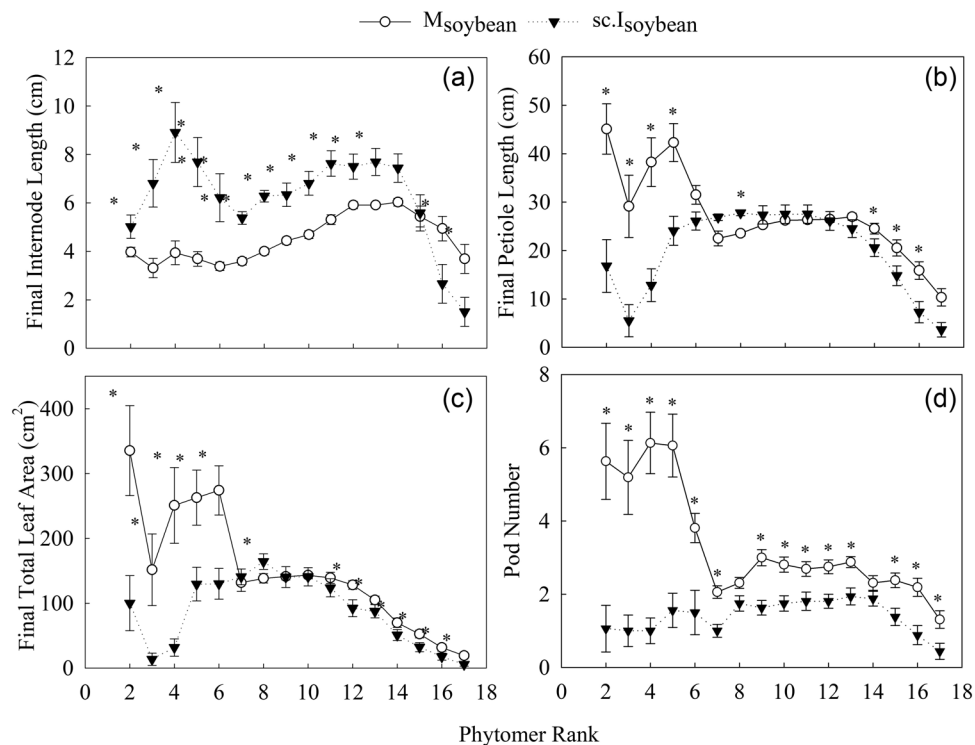


FIGURE 5 Soybean plant architecture analysis across phytomer ranks during the 2019 growing season. Mean final internode length (a), petiole length (b), total leaf area of trifoliolate (c), and pod number (d) versus phytomer rank at full seed for soybean in monoculture (M_{soybean} = white circle) and solar corridor intercrop ($sc.I_{\text{soybean}}$ = black triangle). Asterisks indicate a significant difference within phytomer rank at $\alpha = 0.1$ when present. Phytomer 1 (unifoliolate leaves) was not measured due to advanced senescence at the time of sampling. Error bars and replicates are as in Figure 3.

only significantly affected by DAE (Appendix Table A.1). At canopy closure, $sc.I_{\text{soybean}}$ intercepted ~45% of the incident light available within the solar corridor maize rows, whereas M_{soybean} intercepted 90% of downwelling incident light (Figure 7b). Thus, light interception fractions of M_{soybean} normalized to the plant density of intercropped soybean ($M_{\text{soybean}}^{*0.5}$) indicates 45% light interception at canopy closure and agrees with the nonsignificant cropping effect on soybean plant leaf area (Figure 7b).

Differences in maize plant leaf area were apparent after maize reached seven leaves, where both systems of maize in the solar corridor arrangement expressed a decrease compared with M_{maize} (Figure 7c) where only $sc.I_{\text{maize}}$ was significantly lower (Appendix Table A.1). Light interception measurements matched the leaf area response by a similar deviation between systems (Figure 7d). At canopy closure, M_{maize} intercepted 80% of downwelling incident light, whereas $sc.M_{\text{maize}}$ and $sc.I_{\text{maize}}$ canopies intercepted around 70% (Figure 7d).

3.8 | The solar corridor intercrop system had negative impacts on the seasonal light-use efficiencies of both crops in 2019

The seasonal light interception fraction (ϵ_i) for maize in both solar corridor systems was similar and significantly lower than M_{maize}

($p < 0.001$, Table 4). Only $sc.I_{\text{maize}}$ had a significant reduction in seasonal conversion efficiency (ϵ_c) compared with both maize monoculture systems by the accumulation of less biomass MJ m^{-2} ($p < 0.05$, Table 4 and Figure 8b). Under the area of the intercrop system, the ϵ_i for $sc.I_{\text{soybean}}$ was no different than $M_{\text{soybean}}^{*0.5}$, but ϵ_c for $sc.I_{\text{soybean}}$ was lower than $M_{\text{soybean}}^{*0.5}$ ($p < 0.1$, Table 4 and Figure 8a).

The combined seasonal performance of both maize and soybean in the intercrop system ($sc.I_{\text{maize+soybean}}$) was compared against the two maize monoculture systems (Figure 9). The M_{soybean} system was excluded from comparisons due to the inherently different functional and structural characteristics compared to systems involving maize. The addition of soybean in the intercrop increased LAI more than both maize monoculture systems ($p < 0.1$) and ϵ_i compared with the $sc.M_{\text{maize}}$ system only ($p < 0.001$). However, biomass at silking and ϵ_c were higher for M_{maize} than the intercrop ($p < 0.1$). Biomass at silking was also higher for M_{maize} than $sc.M_{\text{maize}}$ ($p < 0.01$). No differences in end-of-season stover were found ($p > 0.1$).

3.9 | Intercrop grain yield was lower in each experimental year and averaged across years

Compared with each respective monoculture system in 2019, the intercrop reduced maize grain yield by 34% at equal maize plant density

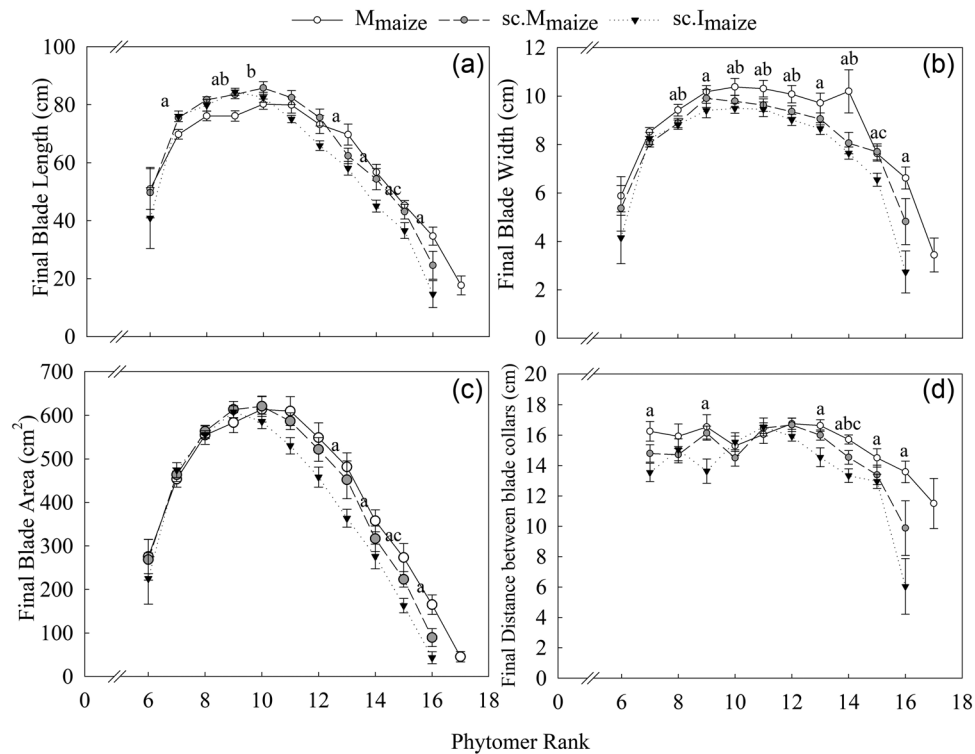


FIGURE 6 Maize plant architecture analysis across phytomer ranks during the 2019 growing season. Mean final blade length (a), final blade width (b), final blade area (c), and final distance between blade collars (d) versus phytomer rank at silking for maize in monoculture (M_{maize} = white circle), solar corridor monoculture ($sc.M_{maize}$ = grey circle) and solar corridor intercrop ($sc.I_{maize}$ = black triangle). Letters indicate significant differences between cropping systems within a phytomer rank at $\alpha = 0.1$ when present where $a = M_{maize} - sc.I_{maize}$, $b = M_{maize} - sc.M_{maize}$ and $c = sc.M_{maize} - sc.I_{maize}$. Phytomers 1–5 were not measured due to their advanced senescence at the time of sampling. Error bars and replicates are as in Figure 3.

($p < 0.05$) and soybean grain yield by 78% at half the soybean plant density (56% lower than $M_{soybean}^{*0.5}$ [$p < 0.01$, Table 4]). In comparison with $sc.M_{maize}$, no difference in intercrop maize grain yield was found ($p = 0.32$, Table 4). Compared with M_{maize} , the $sc.M_{maize}$ system had no difference in grain yield but was more variable ($p = 0.22$, Table 4). No differences were found in HI ($p = 0.83$) and seed mass ($p = 0.16$) between maize cropping systems, whereas $sc.I_{soybean}$ had lower HI ($p < 0.05$) but similar seed mass to $M_{soybean}$ ($p = 0.71$; Table 4).

In 2020, decreasing maize plant density in the solar corridor intercrop compared with the standard M_{maize} system decreased maize grain yields ($p < 0.1$), whereas at equal maize plant density, no differences in maize grain yield were found, including between $sc.M_{maize}$ and M_{maize} . However, the grain yield of $sc.I_{soybean}$ remained lower than $M_{soybean}$ and $M_{soybean}^{*0.5}$ across maize plant density treatments ($p < 0.1$). No differences were found in maize and soybean HI across cropping systems ($p > 0.1$) and the seed mass of maize and soybean increased with decreasing maize plant density compared to each respective monoculture system ($p < 0.1$, Appendix Table A.2).

Grain yields from 2019 and grain yields from the systems with the highest maize plant density in 2020 were used to calculate the 2-year average grain yield, $LER_{average}$ and $LER_{rotation}$ (Table 5). Grain yields of $sc.I_{maize}$ and $sc.I_{soybean}$ were significantly lower than their respective monocultures by 31% and 77%, respectively ($p < 0.01$).

The land-use efficiency of the solar corridor intercrop was lower on average and in rotation compared to the standard monoculture systems by $9\% \pm 0.05\%$ and $19\% \pm 0.04$, respectively.

4 | DISCUSSION

The solar corridor intercrop system was hypothesized to improve light capture and increase or sustain maize yields with the additional forage benefit or grain yield from the intercropped legume enhancing ecosystem services beyond the standard monoculture systems of the Midwest, USA (Deichman, 2000; Kremer, 2016; Kremer & Deichman, 2014b). This study evaluated aboveground plasticity within the physiological and architectural dimensions of the intercrop system and its consequences for light-use across biological scales under high maize plant density in 2019 and the impact of reducing maize plant density on yield in 2020. We show that both intercropped species invested in aboveground physiological and architectural plasticity, and high maize plant density produced the greatest yields in solar corridor monoculture and intercrop systems. However, the collective performance of both crops in the intercrop was suboptimal, despite an increase in LAI and maintenance of ϵ_i by the addition of soybean. On average, the intercrop resulted in a 31% and 77% grain yield

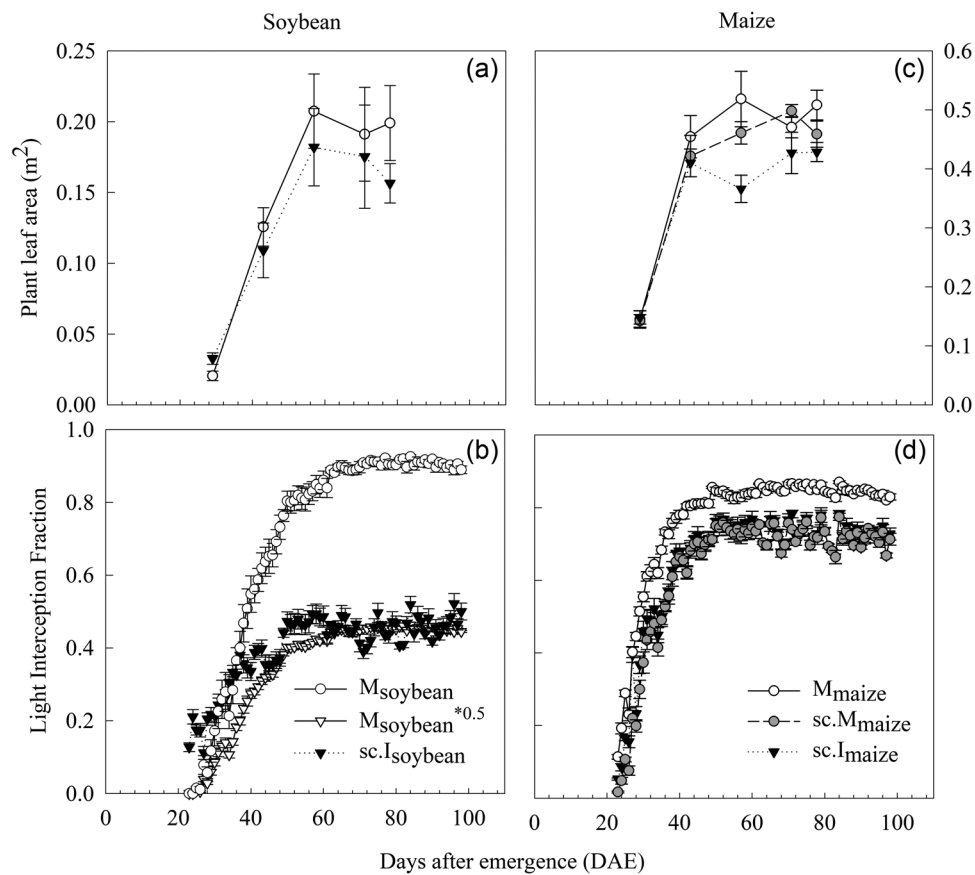


FIGURE 7 Plant leaf area and daily light interception fractions across days after emergence (DAE) during the 2019 growing season. Mean leaf area per plant (a,b) and light interception fractions (c,d) for soybean and maize. Symbols are as in Figure 6 for maize and Figure 5 for soybean with the addition of M_{soybean} under the area of the intercrop ($M_{\text{soybean}}^{*0.5}$ = white triangle). Error bars and replicates are as in Figure 3.

TABLE 4 Seasonal canopy level processes related to the Monteith equation (Monteith & Moss, 1977), grain yield, HI and seed mass of maize and soybean cropping systems in the 2019 growing season

Cropping system	ϵ_i	ϵ_c	Grain yield (g m^{-2})	HI	Seed mass ($\text{g [100 seeds]}^{-1}$)
M_{maize}	0.77 ± 0.01	0.020 ± 0.001	963.54 ± 24.86	0.57 ± 0.03	35.92 ± 0.83
$sc.M_{\text{maize}}$	$0.64^* \pm 0.01$	0.021 ± 0.001	787.89 ± 105.48	0.58 ± 0.02	36.83 ± 2.06
$sc.I_{\text{maize}}$	$0.65^* \pm 0.01$	$0.017^{**} \pm 0.001$	$639.41^* \pm 47.23$	0.57 ± 0.01	33.07 ± 1.13
Soybean expected^a and observed^b yield per m^2 of intercrop					
M_{soybean}	0.70 ± 0.02	0.012 ± 0.001	266.23 ± 23.49	0.57 ± 0.02	18.52 ± 0.47
Expected $M_{\text{soybean}}^{*0.5}$	0.35 ± 0.01	0.012 ± 0.001	133.12 ± 11.74	–	–
Observed $sc.I_{\text{soybean}}$	0.40 ± 0.04	$0.009^* \pm 0.001$	$59.24^* \pm 7.64$	$0.51^* \pm 0.02$	18.73 ± 0.52

Note: Growing season means with ± 1 SE ($n = 4$) are reported for seasonal interception efficiency (ϵ_i), conversion efficiency (ϵ_c), grain yield at physiological maturity, harvest index and mass per 100 seeds. Significant differences compared with M systems within species are indicated with a single asterisk and differences compared with both M and sc.M systems are indicated with a double asterisk at $\alpha = 0.1$.

Abbreviation: HI, harvest index.

^aThe expected yield is the absolute yield of M_{soybean} multiplied by the relative density of soybean in the intercrop (0.5) under the null hypothesis that individual soybean plants have the same yield in intercrop as in the monoculture.

^bThe observed $sc.I_{\text{soybean}}$ is the ϵ_i , ϵ_c and grain yield per unit area of intercropping.

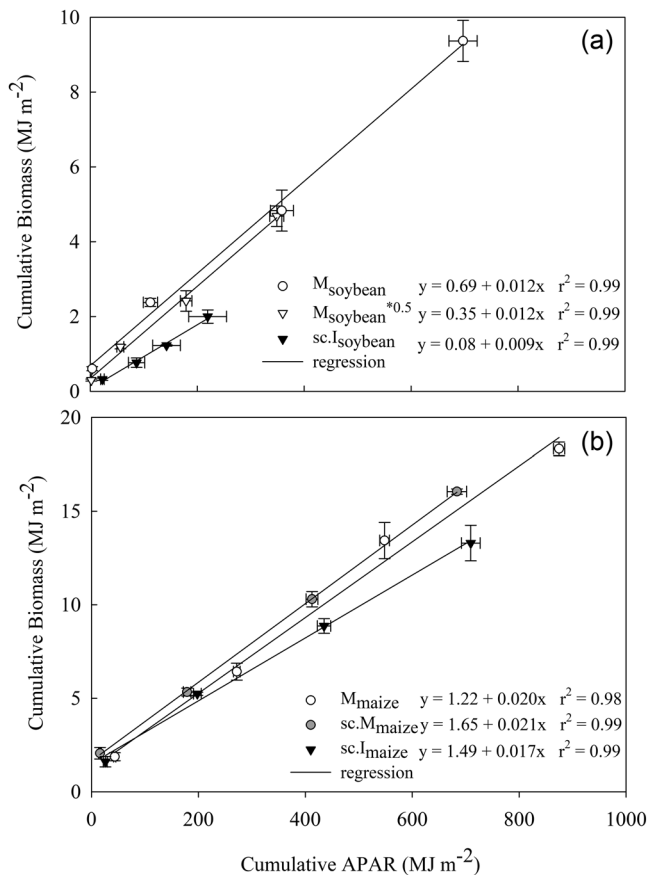


FIGURE 8 Linear regressions for the calculation of light conversion efficiency (ϵ_c) during the 2019 growing season. Data points represent cropping system means (± 1 SE error bar; $n = 4$) where M_{soybean} values were multiplied by the area of intercrop ($M_{\text{soybean}}^{*0.5}$ = white triangle). Solid black lines represent least-squared regression between cumulative dry biomass and absorbed photosynthetically active radiation (APAR) for soybean (a) and maize (b). The slope of each line is the conversion efficiency (ϵ_c). Symbols are as in Figure 5 for soybean and Figure 6 for maize.

decrease of maize and soybean, respectively, compared with their respective monoculture systems. This led to an LER_{average} of 0.91 ± 0.05 (1 SE), suggesting a decrease in land-use efficiency where 9% more land area is needed for the intercrop to achieve the same yields as the monoculture systems of the Midwest, USA. If the intercrop were to replace the maize monoculture in the annual rotations (LER_{rotation}), land-use efficiency would decrease further to 19%. This indicates that uncoordinated investment in aboveground plasticity by each component crop in an additive and simultaneous design under high maize plant density does not establish light complementarity, leading to a yield disadvantage.

4.1 | Maize response

For the maize cultivar evaluated in this study, $sc.I_{\text{maize}}$ plants displayed the lowest structural dimensions (Figure 6a–c), including

plant height (Appendix Figure A.6B), and accumulated the lowest aboveground biomass (Figure 8b, and Appendix Figure A.7B and A.8B). Therefore, $sc.I_{\text{maize}}$ showed a decrease in ϵ_c compared with both $sc.M_{\text{maize}}$ and M_{maize} (Table 4), which suggests that interspecific competition between maize and soybean occurred. In response to interspecific competition, the $sc.I_{\text{maize}}$ plants invested in physiological plasticity, evidenced by a seasonal 10% increase in SLA and a 13% reduction in photoprotective carotenoids compared with M_{maize} plants (Table 2). However, the decrease in total chl content for $sc.I_{\text{maize}}$ may have hindered such investments from maintaining ϵ_c , despite no impacts on photosynthetic rate and biomass allocation to grain yield (Tables 2–4). Furthermore, the reduction in $sc.I_{\text{maize}}$ plant height and blade length compared with M_{maize} plants suggests there was no investment in architectural plasticity (Figure 6 and Appendix Figure A.6). It has been argued that domestication has reduced architectural plasticity through selection for yield at high density as the response reduces biomass allocation to yield (Carriedo et al., 2016; Wille et al., 2017). However, architectural plasticity has not been fully eliminated and can be advantageous against weed suppression (Carriedo et al., 2016). Therefore, selecting a modern maize cultivar that favours architectural plasticity rather than physiological plasticity could improve maize yields in the solar corridor intercrop system under high maize plant density.

A previous study identified 21 maize hybrids out of 200 as promising candidates for the $sc.M_{\text{maize}}$ system and stressed the need to select appropriate maize hybrids for optimal performance (Deichman & Kremer, 2019). However, the study only considered nongenetically modified maize hybrids with early release dates not representative of modern hybrids used in the Midwest today. Another study that conducted multiple years of experiments also reported an underperformance in both the solar corridor monoculture and intercrop systems concerning two modern hybrid maize cultivars (Nelson, 2014). Although our study only considered one modern maize hybrid, a reduction in yield for both $sc.M_{\text{maize}}$ and $sc.I_{\text{maize}}$ compared with that of the standard maize monoculture system was also found, and reducing maize plant density does not minimize maize yield losses (Appendix Table A.2). Historic yield trends of maize hybrids in the Midwest have been attributed to increasing population density and changes in belowground architecture may have had a more direct role than aboveground architecture (Hammer et al., 2009). Efforts to characterize belowground plasticity in modern maize hybrids may be more effective at improving the solar corridor intercrop system, which would complement the evidence that the $sc.M_{\text{maize}}$ system can promote soil quality (Kremer & Deichman, 2014a).

4.2 | Soybean response

On average the $sc.I_{\text{maize}}$ provided 60%–80% of incident light for $sc.I_{\text{soybean}} \pm 2$ h from solar noon in 2019 (Figure 3). To adapt, the soybean cultivar used in this study invested in both physiological and

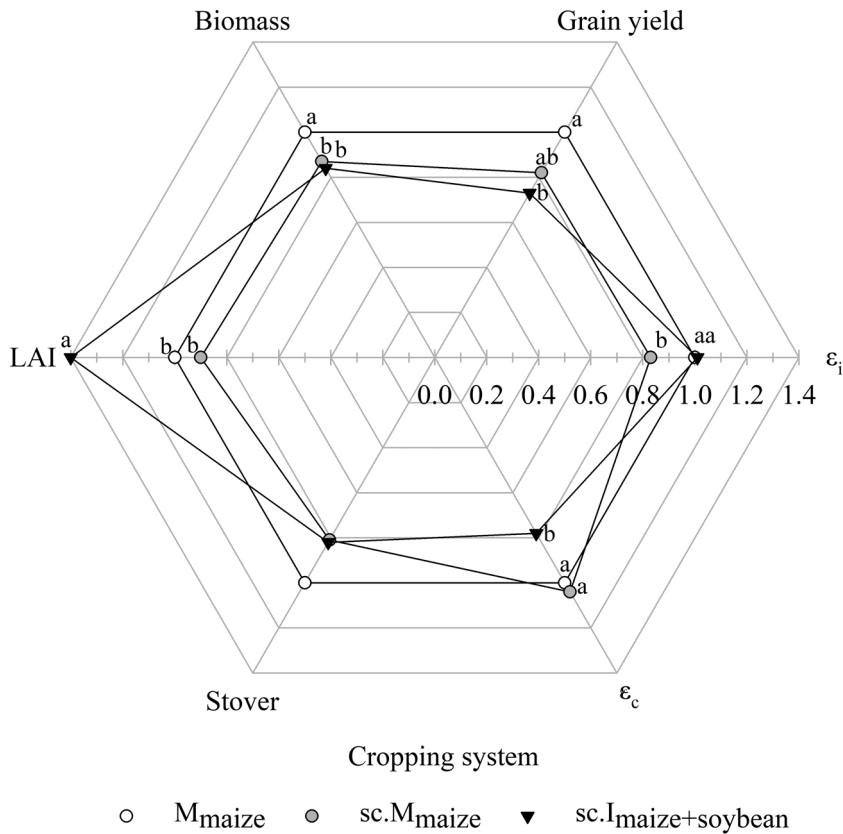


FIGURE 9 Radar plot of cropping system performance in 2019. Mean ($n = 4$) seasonal performance of maize in monoculture (M_{maize} , white circle), maize solar corridor monoculture ($sc.M_{maize}$, grey circle) and the combined seasonal performance of maize and soybean in the solar corridor intercrop ($sc.I_{maize+soybean}$, black triangle). Parameter means were normalized and are relative to the M_{maize} system which was set to 1. Parameters include grain yield and stover at physiological maturity, biomass (at silking and full seed reproductive stages for maize and soybean, respectively), leaf area index (LAI), seasonal interception efficiency (ϵ_i) and conversion efficiency (ϵ_c). Letters indicate significant differences within the parameter at $\alpha = 0.1$.

TABLE 5 Two-year average grain yield and LER between the 2019 and 2020 growing seasons

	Monoculture		$M_{soybean}$	Intercrop		Total	LER	
	M_{maize}	$sc.M_{maize}$		$sc.I_{maize}$	$sc.I_{soybean}$		$LER_{average}$	$LER_{rotation}$
Two-year average grain yield ($g\ m^{-2}$)	$934.47a \pm 24.18$	$834.72a \pm 61.40$	288.71 ± 12.33	$640.26b \pm 40.85$	66.40^*	706.66 ± 44.81	0.91 ± 0.05	0.81 ± 0.04

Note: The 2-year yield averages ($n = 3$, ± 1 SE) between 2019 and 2020 are reported. Letters indicate significant differences within maize and an asterisk indicates significant differences within soybean at $p < 0.1$. $LER_{average}$ was calculated by using the above grain yield values and Equation 3. $LER_{rotation}$ was calculated by using grain yield values in Table 4 and Appendix Table A.2 and Equation 4 ($n = 3$, ± 1 SE).

Abbreviation: LER, land equivalent ratio.

architectural plasticity. In the early phase of vegetative growth, plasticity in leaf area conferred a transient competitive advantage for $sc.I_{soybean}$ relative to $M_{soybean}$ by higher interception fractions (Figure 7b). During the canopy closure phase, $sc.I_{soybean}$ plants were taller and less branched (Figure 5 and Appendix Figure A.6A and A.9) with similar plant leaf area to $M_{soybean}$ plants (Figure 7a). Thus, no differences in ϵ_i under the intercrop area were found, despite $M_{soybean}$ plants exhibiting a higher spatial clustering of leaves at the lower phytomer ranks by branching (Figure 5c and Appendix Figure A.9). However, the physiological plasticity of $sc.I_{soybean}$ leaves by maximizing net carbon gain through higher SLA, expression of more accessory pigment chlorophyll b and fewer carotenoids while maintaining chl content, did not sustain a similar ϵ_c to that in $M_{soybean}$ (Tables 2 and 4). Moreover, biomass allocation to grain yield was reduced even though seed mass was maintained (Figure 5d and Table 4). In 2020, decreasing the maize plant density did not increase

$sc.I_{soybean}$ yield significantly (Appendix Table A.2) but the increase suggests that the intensity of interspecific competition eased slightly.

The occurrence of both shade responses supports the hypothesis that the molecular regulatory components from shade detection to phenotypic output may be shared in soybean (Gommers et al., 2013; Gong et al., 2015). Efforts to identify the genetic factors and redirect the response solely to physiological plasticity could be an attractive approach for legumes under intercropping, as architectural plasticity is likely to be inefficient given the physiological and structural dominance of most cereals. This argument is further supported by a previous study considering a different simultaneous maize and soybean intercrop at regular row spacing and lower maize plant density, which concluded that architectural plasticity does not contribute to a yield advantage (C. Li et al., 2020). However, similar to maize, only one modern cultivar of soybean was investigated in this study, which has been bred for high performance in

monocultures under high light. Screening for plastic responses in older soybean cultivars and its wild ancestor *Glycine soja* would provide more evidence of its potential in the solar corridor intercrop.

4.3 | Implications, the broader context and considerations for future studies

Beyond competition for light, the relative land-use advantage of intercropping decreases with high N fertilizer input, particularly when cereals and legumes are sown simultaneously. This phenomenon occurs because competition for N increases through weakening the biological capture of atmospheric N by the legume (Hauggaard-Nielsen & Jensen, 2001; S. Li et al., 2020; Yu et al., 2015). If a plant displays reduced growth in intercropping due to competition for one or more resources, its acquisition for other resources may also decrease, as the plant functions as a unified system. Such negative feedback obscures the identification of the original drivers of competition (Tang et al., 2020). As this study explored a simultaneous cereal/legume intercrop with a high N input and only considered light competition, the conclusion that the lack of complementarity in light capture traits was solely responsible for the yield losses may need further examination.

Moreover, interspecific competition can be intensified by simultaneous planting of component crops compared with relay intercrop systems, where the co-growth period is shortened by different planting dates for each crop (Xu et al., 2020). A global meta-analysis suggested that the most significant absolute yield gains in high-input intercrop systems were achieved by maize and legumes arranged in multirow strips with considerable temporal niche differentiation (C. Li et al., 2020). Although designing a multirow relay intercrop system that can be mechanically managed with existing machinery in the Midwest may be more favourable in terms of delivering higher yield gains, the solar corridor intercrop system offers to replace the maize monoculture in annual rotation while potentially increasing regulating ecosystem services through the addition of the legume. Further, a relay system may not be ideal for the solar corridor, wheat strips sown before solar corridor maize was the least productive system compared to both sc.M_{maize} and standard M_{maize} systems (Nelson, 2014). In addition, relay intercropping increases the occurrence of mechanized planting. As the Midwest is expected to have more extreme weather events with a higher amount of rainfall in the spring, improving the performance of a simultaneous solar corridor intercrop design may be well-favoured by farmers under a limited number of viable planting days (Hayhoe et al., 2018; Tomasek et al., 2015, 2017).

Given the large yield disadvantage reported in this study for both crops on average and in rotation, little incentive to invest in improving the solar corridor intercrop system may be argued. However, this study only addressed the response of single cultivar for each crop, and despite the inclusion of data from two growing seasons, the weather-induced damage likely impacted the yield results (Appendix Table A.2). Further examination investigating the yield response of multiple elite and ancestral cultivars of maize and soybean, or other short stature crops, across various locations in the

Midwest would narrow down those cultivars that perform best within the solar corridor intercrop design. Architectural and physiological evaluations of the better performing cultivars can then be conducted to then identify which traits and plastic trait responses suit the solar corridor intercrop system.

Furthermore, the detailed architectural and physiological data presented in this study could be used to parameterize a mechanistic functional-structural plant (FSP) model to identify those better suited traits at a faster pace than conducting multiple field trials. Such models simulate plant growth in three-dimensions at the organ level and have proven to be a valuable tool in simulating crops systems to understand the contribution of individual traits to plant performance (Evers et al., 2019; Gaudio et al., 2019). Individual traits can be varied one by one per simulation scenario, and the effect of each plastic trait on plant performance can be quantified separately across monoculture and intercrop configurations. So far, only descriptive FSP models have been used to quantify the contribution of plasticity to light interception in intercrops (Barillot et al., 2014; Li et al., 2021; Zhu et al., 2015). The development of a mechanistic FSP model including photosynthesis and assimilate distribution according to light interception and organ sink demands is a necessary step forward to strengthen the understanding between plasticity and yield in the solar corridor intercrop.

ACKNOWLEDGMENTS

This work was funded by the USDA to the Global Change and Photosynthesis Research Unit of the USDA Agricultural Research Service. Mention of trade names or commercial products in this publication is solely to provide specific information and does not imply recommendation or endorsement by the U.S. Department of Agriculture. USDA is an equal opportunity provider and employer. Any opinions, findings, and conclusions or recommendations expressed in this publication are those of the author(s) and do not necessarily reflect the views of the U.S. Department of Agriculture. The authors thank Tim Mies, Ben Harbaugh, Ben Thompson, Ron Edquiang and Trace Elliot for their management and assistance of the Energy Farm Facility and preparations of the field for this project. The authors also thank Erin Fisher, Bethany Blakely, Matt Siebers, Scott Swanson, Oviya Sougoumarane, Christy Gibson, Katie Bowman, Brett Feddersen, Xiangmin Sun and Evan Dracup for their assistance with data collection and sensor maintenance. The authors also thank Adam Davis, Will Glazik, Bob Recker and LeRoy Deichman for their guidance on the solar corridor concept. Lastly, the authors thank Elizabeth Ainsworth, Don Ort and Adam Davis for their scientific advice throughout the development of this manuscript.

DATA AVAILABILITY STATEMENT

The data that support the findings of this study are available from the corresponding author upon reasonable request.

ORCID

Elena A. Pelech  <http://orcid.org/0000-0001-5084-324X>

Jochem B. Evers  <http://orcid.org/0000-0002-3956-0190>

David W. Drag  <http://orcid.org/0000-0002-9542-9672>

Peng Fu  <http://orcid.org/0000-0003-1568-1518>

Carl J. Bernacchi  <http://orcid.org/0000-0002-2397-425X>

REFERENCES

- Abels, F., Boyer, J., Kessel, B., Kessel, H., Johnson, J. & Teachout, C. (2019). Planting Corn in 60-in. Row Widths for Interseeding Cover Crops. Practical Farmers of Iowa Cooperators' Program Research Report (In press).
- Barillot, R., Escobar-Gutiérrez, A.J., Fournier, C., Huynh, P. & Combes, D. (2014) Assessing the effects of architectural variations on light partitioning within virtual wheat-pea mixtures. *Annals of Botany*, 114, 725–737. Available from: <https://doi.org/10.1093/aob/mcu099>
- Bellasio, C., Beerling, D.J. & Griffiths, H. (2015) An excel tool for deriving key photosynthetic parameters from combined gas exchange and chlorophyll fluorescence: theory and practice. *Plant, Cell & Environment*, 39, 1180–1197. Available at <https://doi.org/10.1111/pce.12560>
- Bellasio, C., Beerling, D.J. & Griffiths, H. (2016) Deriving C4 photosynthetic parameters from combined gas exchange and chlorophyll fluorescence using an Excel tool: theory and practice. *Plant, Cell & Environment*, 39, 1164–1179. Available from: <https://doi.org/10.1111/pce.12626>
- Boardman, N.K. (1977) Comparative photosynthesis of sun and shade plants. *Annual Review of Plant Physiology*, 28, 355–377. Available from: <https://doi.org/10.1146/annurev.pp.28.060177.002035>
- Brooker, R.W., Bennett, A.E., Cong, W.F., Daniell, T.J., George, T.S., Hallett, P.D. et al. (2015) Improving intercropping: a synthesis of research in agronomy, plant physiology and ecology. *New Phytologist*, 206, 107–117. Available from: <https://doi.org/10.1111/nph.13132>
- Cardinale, B.J., Wright, J.P., Cadotte, M.W., Carroll, I.T., Hector, A., Srivastava, D.S. et al. (2007) Impacts of plant diversity on biomass production increase through time because of species complementarity. *Proceedings of the National Academy of Sciences*, 104, 18123–18128. Available from: <https://doi.org/10.1073/pnas.0709069104>
- Carriedo, L.G., Maloof, J.N., & Brady, S.M. (2016) Molecular control of crop shade avoidance. *Current Opinion in Plant Biology*, 30, 151–158. Available from: <https://doi.org/10.1016/j.pbi.2016.03.005>
- Cong, W.F., Hoffland, E., Li, L., Six, J., Sun, J.H., Bao, X.G. et al. (2015) Intercropping enhances soil carbon and nitrogen. *Global Change Biology*, 21, 1715–1726. Available from: <https://doi.org/10.1111/gcb.12738>
- Deichman, C.L. (2000) *Plant Arrangement for improving crop yields*. U.S. Patent No. 6,052,941. U.S. Patent and Trademark Office.
- Deichman, C.L. & Kremer, R.J. (2019) *The Solar Corridor Crop System*. Elsevier: Academic Press.
- Evers, J.B., van der Werf, W., Stomph, T.J., Bastiaans, L. & Anten, N.P.R. (2019) Understanding and optimizing species mixtures using functional-structural plant modelling. *Journal of Experimental Botany*, 70, 2381–2388. Available from: <https://doi.org/10.1093/jxb/ery288>
- FAO. (2020). World Food and Agriculture - Statistical Yearbook 2020. Rome. [10.4060/cb1329en](https://doi.org/10.4060/cb1329en)
- Foley, J.A., Ramankutty, N., Brauman, K.A., Cassidy, E.S., Gerber, J.S., Johnston, M. et al. (2011) Solutions for a cultivated planet. *Nature*, 478, 337–342. Available from: <https://doi.org/10.1038/nature10452>
- Gaudio, N., Escobar-Gutiérrez, A.J., Casadebaig, P., Evers, J.B., Gérard, F., Louarn, G. et al. (2019) Current knowledge and future research opportunities for modeling annual crop mixtures. A review. *Agronomy for Sustainable Development*, 39, 20. Available from: <https://doi.org/10.1007/s13593-019-0562-6>
- Givnish, T. (1988) Adaptation to sun and shade: a Whole-Plant perspective. *Functional Plant Biology*, 15, 63–92. Available from: <https://doi.org/10.1071/pp9880063>
- Godfray, H.C.J. & Garnett, T. (2014) Food security and sustainable intensification. *Philosophical Transactions of the Royal Society, B: Biological Sciences*, 369, 20120273. Available from: <https://doi.org/10.1098/rstb.2012.0273>
- Gommers, C.M.M., Visser, E.J.W., Onge, K.R.S., Voesenek, L.A.C.J. & Pierik, R. (2013) Shade tolerance: when growing tall is not an option. *Trends in Plant Science*, 18, 65–71. Available from: <https://doi.org/10.1016/j.tplants.2012.09.008>
- Gong, W.Z., Jiang, C.D., Wu, Y.S., Chen, H.H., Liu, W.Y. & Yang, W.Y. (2015) Tolerance vs. avoidance: two strategies of soybean (*Glycine max*) seedlings in response to shade in intercropping. *Photosynthetica*, 53, 259–268. Available from: <https://doi.org/10.1007/s11099-015-0103-8>
- Hammer, G.L., Dong, Z., McLean, G., Doherty, A., Messina, C., Schussler, J. et al. (2009) Can changes in canopy and/or root system architecture explain historical maize yield trends in the U.S. Corn Belt? *Crop Science*, 49, 299–312. Available from: <https://doi.org/10.2135/cropsci2008.03.0152>
- Hauggaard-Nielsen, H. & Jensen, E.S. (2001) Evaluating pea and barley cultivars for complementarity in intercropping at different levels of soil N availability. *Field Crops Research*, 72, 185–196. Available from: [https://doi.org/10.1016/s0378-4290\(01\)00176-9](https://doi.org/10.1016/s0378-4290(01)00176-9)
- Hayhoe, K., Wuebbles, D.J., Easterling, D.R., Fahey, D.W., Doherty, S., Kossin, J.P. et al. (2018) Our changing climate. Impacts, risks, and adaptation in the United States, The Fourth National Climate Assessment, Volume II. <https://doi.org/10.7930/NCA4.2018.CH2>
- Koester, R.P., Skoneczka, J.A., Cary, T.R., Diers, B.W. & Ainsworth, E.A. (2014) Historical gains in soybean (*Glycine max* merr.) seed yield are driven by linear increases in light interception, energy conversion, and partitioning efficiencies. *Journal of Experimental Botany*, 65, 3311–3321. Available from: <https://doi.org/10.1093/jxb/eru187>
- Kremer, R.J. (2016) The solar corridor: a new paradigm for sustainable crop production. *Advances in Plants & Agriculture Research*, 4, 273–274. Available from <https://doi.org/10.15406/apar.2016.04.00136>
- Kremer, R.J. & Deichman, C.L. (2014a) Soil quality and the solar corridor crop system. *Agronomy Journal*, 106, 1853–1858. Available from: <https://doi.org/10.2134/agronj13.0508>
- Kremer, R.J. & Deichman, C.L. (2014b) Introduction: the solar corridor concept. *Agronomy Journal*, 106, 1817–1819. Available from: <https://doi.org/10.2134/agronj14.0291>
- Li, C., Hoffland, E., Kuyper, T.W., Yu, Y., Zhang, C., Li, H. et al. (2020) Syndromes of production in intercropping impact yield gains. *Nature Plants*, 6, 653–660. Available from: <https://doi.org/10.1038/s41477-020-0680-9>
- Li, L., Tilman, D., Lambers, H. & Zhang, F.S. (2014) Plant diversity and overyielding: insights from belowground facilitation of intercropping in agriculture. *New Phytologist*, 203, 63–69. Available from: <https://doi.org/10.1111/nph.12778>
- Li, S., Evers, J.B., Werf, W., Wang, R., Xu, Z., Guo, Y. et al. (2020) Plant architectural responses in simultaneous maize/soybean strip intercropping do not lead to a yield advantage. *Annals of Applied Biology*, 177(2), 195–210. Available from: <https://doi.org/10.1111/aab.12610>
- Li, S., van der Werf, W., Zhu, J., Guo, Y., Li, B., Ma, Y. et al. (2021) Estimating the contribution of plant traits to light partitioning in simultaneous maize/soybean intercropping. *Journal of Experimental Botany*, 72(Issue 10), 3630–3646. Available from: <https://doi.org/10.1093/jxb/erab077>
- Lichtenthaler, H.K. (1987) Chlorophylls and carotenoids: pigments of photosynthetic biomembranes. *Methods in Enzymology*, 148, 350–382. Available from: [https://doi.org/10.1016/0076-6879\(87\)48036-1](https://doi.org/10.1016/0076-6879(87)48036-1)

- Loreau, M. & Hector, A. (2001) Partitioning selection and complementarity in biodiversity experiments. *Nature*, 412, 72–76. Available from: <https://doi.org/10.1038/35083573>
- Monteith, J.L. & Moss, C.J. (1977) Climate and the efficiency of crop production in Britain. *Philosophical Transactions of the Royal Society of London. B, Biological Sciences*, 281, 277–294. Available from: <https://doi.org/10.1098/rstb.1977.0140>
- Nelson, K.A. (2014) Corn yield response to the solar corridor in upstate Missouri. *Agronomy Journal*, 106, 1847–1852. Available from: <https://doi.org/10.2134/agnonj2012.0326>
- Niklaus, P.A., Baruffol, M., He, J.S., Ma, K. & Schmid, B. (2017) Can niche plasticity promote biodiversity–productivity relationships through increased complementarity? *Ecology*, 98, 1104–1116. Available from: <https://doi.org/10.1002/ecy.1748>
- Pinheiro, J., Bates, D., DebRoy, S., Sarkar, D. & R. Core Team. 2021. nlme: linear and nonlinear mixed effects models. R package version 3.1-152. Available at: <https://CRAN.R-project.org/package=nlme>
- Porra, R.J., Thompson, W.A. & Kriedemann, P.E. (1989) Determination of accurate extinction coefficients and simultaneous equations for assaying chlorophylls a and b extracted with four different solvents: verification of the concentration of chlorophyll standards by atomic absorption spectroscopy. *Biochimica et Biophysica Acta (BBA) - Bioenergetics*, 975, 384–394. Available from: [https://doi.org/10.1016/s0005-2728\(89\)80347-0](https://doi.org/10.1016/s0005-2728(89)80347-0)
- R Core Team. (2021) R: A language and environment for statistical computing. Vienna, Austria: R Foundation for Statistical Computing. <http://www.R-project.org/>
- Russell, V. L., (2021) Emmeans: Estimated Marginal Means, aka Least-Squares Means. R package version 1.6.2-1. Available at: <https://CRAN.R-project.org/package=emmeans>
- Soil Survey Staff. (2015) Natural Resources Conservation Service, United States Department of Agriculture. Official Soil Series Descriptions. Retrieved from https://www.nrcs.usda.gov/wps/portal/nrcs/detail/soils/scientists/?cid=nrcs142p2_053587
- Tang, X., Zhang, C., Yu, Y., Shen, J., van der Werf, W. & Zhang, F. (2020) Intercropping legumes and cereals increases phosphorus use efficiency: a meta-analysis. *Plant and Soil*, 460, 89–104. Available from: <https://doi.org/10.1007/s11104-020-04768-x>
- Tilman, D., Balzer, C., Hill, J. & Befort, B.L. (2011) Global food demand and the sustainable intensification of agriculture. *Proceedings of the National Academy of Sciences*, 108, 20260–20264. Available from: <https://doi.org/10.1073/pnas.1116437108>
- Tilman, D., Clark, M., Williams, D.R., Kimmel, K., Polasky, S. & Packer, C. (2017) Future threats to biodiversity and pathways to their prevention. *Nature*, 546, 73–81. Available at <https://doi.org/10.1038/nature22900>
- Tomasek, B.J., Williams, M.M. & Davis, A.S. (2015) Optimization of agricultural field workability predictions for improved risk management. *Agronomy Journal*, 107, 627–633. Available from: <https://doi.org/10.2134/agnonj14.0393>
- Tomasek, B.J., Williams, M.M. & Davis, A.S. (2017) Changes in field workability and drought risk from projected climate change drive spatially variable risks in Illinois cropping systems. *PLoS One*, 12, e0172301. Available from: <https://doi.org/10.1371/journal.pone.0172301>
- Valladares, F. & Niinemets, Ü. (2008) Shade tolerance, a key plant feature of complex nature and consequences. *Annual Review of Ecology, Evolution, and Systematics*, 39, 237–257. Available from: <https://doi.org/10.1146/annurev.ecolsys.39.110707.173506>
- Vandermeer, J.H. (1989) *The Ecology of Intercropping*. Cambridge: Cambridge University Press. Available from: <https://doi.org/10.1017/CBO9780511623523>
- Wille, W., Pipper, C.B., Rosenqvist, E., Andersen, S.B., & Weiner, J. (2017) Reducing shade avoidance responses in a cereal crop. *AoB Plants*, 9, plx039. Available from: <https://doi.org/10.1093/aobpla/plx039>
- Xu, Z., Li, C., Zhang, C., Yu, Y., van der Werf, W., & Zhang, F. (2020) Intercropping maize and soybean increases efficiency of land and fertilizer nitrogen use: a meta-analysis. *Field Crops Research*, 246, 107661. Available from: <https://doi.org/10.1016/j.fcr.2019.107661>
- Yu, Y., Stomph, T.-J., Makowski, D. & van der Werf, W. (2015) Temporal niche differentiation increases the land equivalent ratio of annual intercrops: a meta-analysis. *Field Crops Research*, 184, 133–144. Available from: <https://doi.org/10.1016/j.fcr.2015.09.010>
- Zaeem, M., Nadeem, M., Pham, T.H., Ashiq, W., Ali, W., Gilani, S.S.M. et al. (2019) The potential of corn-soybean intercropping to improve the soil health status and biomass production in cool climate boreal ecosystems. *Scientific Reports*, 9, 13148. Available from: <https://doi.org/10.1038/s41598-019-49558-3>
- Zhang, N., Evers, J.B., Anten, N.P.R. & Marcelis, L.F.M. (2020a) Turning plant interactions upside down: light signals from below matter. *Plant, Cell and Environment*. Available from: <https://doi.org/10.1111/pce.13886>
- Zhang, N., Westreenen, A. van, He, L., Evers, J.B., Anten, N.P.R. & Marcelis, L.F.M. (2020b) Light from below matters: quantifying the consequences of responses to far-red light reflected upwards for plant performance in heterogeneous canopies. *Plant, Cell and Environment*, 44, 102–113. Available from: <https://doi.org/10.1111/pce.13812>
- Zhu, J., Werf, W., Anten, N.P.R., Vos, J. & Evers, J.B. (2015) The contribution of phenotypic plasticity to complementary light capture in plant mixtures. *New Phytologist*, 207, 1213–1222. Available from: <https://doi.org/10.1111/nph.13416>
- Zhu, X.-G., Long, S.P. & Ort, D.R. (2008) What is the maximum efficiency with which photosynthesis can convert solar energy into biomass? *Current Opinion in Biotechnology*, 19, 153–159. Available from: <https://doi.org/10.1016/j.copbio.2008.02.004>
- Zhu, X.-G., Long, S.P. & Ort, D.R. (2010) Improving photosynthetic efficiency for greater yield. *Annual review of plant biology*, 61, 235–261. Available from: <https://doi.org/10.1146/annurev-arplant-042809-112206>

SUPPORTING INFORMATION

Additional supporting information can be found online in the Supporting Information section at the end of this article.

How to cite this article: Pelech, E.A., Evers, J.B., Pederson, T.L., Drag, D.W., Fu, P. & Bernacchi, C.J. (2023) Leaf, plant, to canopy: A mechanistic study on aboveground plasticity and plant density within a maize–soybean intercrop system for the Midwest, USA. *Plant, Cell & Environment*, 46, 405–421. <https://doi.org/10.1111/pce.14487>